

Supplementary Date

Synthesis and evaluation of small molecules bearing a benzyloxy substituent as novel and potent Monoamine Oxidase inhibitors

Jin-Shuai Lan^{1#}, Tong Zhang^{2#}, Yun Liu¹, Yong Zhang¹, Jian-wei Hou¹, Sai-Sai Xie³,
Jing Yang¹, Yue Ding^{1*}, Zhen-zhen Cai^{4*}

1 Experiment Center of Teaching & Learning, Shanghai University of Traditional Chinese Medicine, Shanghai 201203, China;

2 School of Pharmacy, Shanghai University of Traditional Chinese Medicine, Shanghai 201203, China;

3 National Pharmaceutical Engineering Center for Solid Preparation in Chinese Herbal Medicine, Jiangxi University of Traditional Chinese Medicine, Nanchang 330006, China;

4 Experiment Center For Science and Technology, Shanghai University of Traditional Chinese Medicine, Shanghai 201203, China.

* Corresponding author.

* E-mail: zhangtongshutcm@hotmail.com (TZ); dingyue-2001@hotmail.com (YD)

These authors contributed equally to this work.

Biological Evaluation

In vitro inhibition of Monoamine oxidase

Human MAO-A and MAO-B were purchased from Sigma-Aldrich. The capacity of the test compounds to inhibit MAO-A and MAO-B activities was assessed by Amplex Red MAO assay. Briefly, 0.1 mL of sodium phosphate buffer (0.05 M, pH 7.4) containing the test drugs at various concentrations and adequate amounts of recombinant *h*MAO-A or *h*MAO-B required and adjusted to obtain in our experimental conditions the same reaction velocity, i.e., to oxidize (in the control group) the same concentration of substrate: 165 pmol of *p*-tyramine/min (*h*MAO-A: 1.1 µg protein; specific activity: 150nmol of *p*-tyramine oxidized to *p*-hydroxyphenylacetaldehyde/min/mg protein; *h*MAO-B: 7.5 µg protein; specific activity: 22 nmol of *p*-tyramine transformed/min/mg protein) were incubated for 15 min at 37 °C in a flat-black-bottom 96-well microtest plate placed in a dark fluorimeter chamber. After this incubation period, the reaction was started by adding 200 µM (final concentrations) Amplex Red reagent, 1 U/mL horseradish peroxidase, and 1 mM *p*-tyramine. The production of H₂O₂ and consequently, of resorufin, was quantified at 37 °C in a SpectraMax Paradigm (Molecular Devices, Sunnyvale, CA) multi-mode detection platform reader based on the fluorescence generated (excitation, 545 nm; emission, 590 nm). The specific fluorescence emission was calculated after subtraction of the background activity. The background activity was determined from wells containing all components except the *h*MAO isoforms, which were replaced by a sodium phosphate buffer solution (0.05 M, pH 7.4). The percent inhibition was

calculated by the following expression: $(1 - IF_i/IF_c) \times 100$ in which IF_i and IF_c are the fluorescence intensities obtained for hMAO in the presence and absence of inhibitors after subtracting the respective background.

Reversibility and irreversibility study

To determine whether the inhibition of MAO-B by the compound is reversible or irreversible, the time-dependence of inhibition of a selected inhibitor, **9e** and **10e**, were examined. Compounds were allowed to preincubate with recombinant human MAO-B for various periods of time (0, 15, 30, 60 min) at 37 °C in potassium phosphate buffer (0.05 M, pH 7.4). The concentration of compounds were equal to twofold the measured IC_{50} value for the inhibition of MAO-B. The reactions were subsequently diluted twofold to yield a final enzyme concentration of 0.015 mg/mL and concentrations of the compounds are equal to the IC_{50} values. The reactions were incubated at 37 °C for a further 15 min. All measurements were carried out in triplicate and are expressed as mean \pm SD.

Kinetic study of MAO-B inhibition

To obtain of the mechanism of action **10e**, reciprocal plots of 1/velocity versus 1/substrate were constructed at different concentrations of the substrate *p*-tyramine (50–500 μ M). Four different concentrations of **10e** (0, 0.095, 0.19 and 0.38 μ M) were selected for the kinetic analysis of MAO-B inhibition. The plots were assessed by a weighted least-squares analysis that assumed the variance of velocity (v) to be a constant percentage of v for the entire data set. Slopes of these reciprocal plots were then plotted against the concentration of **10e** in a weighted analysis. Data analysis was

performed with Graph Pad Prism 4.03 software (Graph Pad Software Inc.).

Cytotoxicity assay of compounds 9e and 10e

The toxicity effect of compounds **9e** and **10e** on the SH-SY5Y cells was examined. The SH-SY5Y cells were routinely grown at 37 °C in a humidified incubator with 5% CO₂ in Dulbecco's modified Eagle's medium (DMEM) supplemented with 10% bovine calf serum, 100 units/mL penicillin, and 100 units/mL of streptomycin. Cells were subcultured in 96-well plates at a seeding density of 10,000 cells per well and allowed to adhere and grow. When cells reached the required confluence, they were placed into serum-free medium and treated with compounds **9e** and **10e**. 48 Hours later the survival of cells was determined by MTT assay. Briefly, after incubation with 20 µL of MTT at 37 °C for 4 h, living cells containing MTT formazan crystals were solubilized in 200 µL DMSO. The absorbance of each well was measured using a microculture plate reader with a test wavelength of 570 nm and a reference wavelength of 630 nm. Results are expressed as the mean ± SD of three independent experiments.

Molecular Modelling

All calculations and analyses were carried out with Molecular Operating Environment (MOE) program (Chemical Computing Group, Montreal, Canada). The X-ray crystal structures of MAO-B (PDB code 2V61) were applied to build the starting model, which were obtained from the Protein Data Bank (www.rcsb.org). Heteroatoms and water molecules in the PDB files were removed and all hydrogen atoms were subsequently added to the proteins. Compounds **9e**, **10e** and **11e** were

drawn in MOE. The compound was then protonated using the protonate 3D protocol and energy was minimized using the MMFF94x force field in MOE. After the enzymes and compounds were ready for the docking study, compounds were docked into the active site of the protein by the “Triangle Matcher” method. The Dock scoring in MOE software was done using ASE scoring function and forcefield was selected as the refinement method. The best 10 poses of molecules were retained and scored. After docking, the geometry of resulting complex was studied using the MOE’s pose viewer utility.

The modelling studies between compound 10e and compound S1 7-((3-chlorobenzyl)oxy)-4-((methylamino)methyl)-coumarin(Claudia Binda, *J Med Chem.* 2007, 50, 5848-5852.)

The modelling studies between compound **10e** and compound S1 7-((3-chlorobenzyl)oxy)-4-((methylamino)methyl)-coumarin(Claudia Binda, *J Med Chem.* 2007, 50, 5848-5852.) were compared by MOE. As shown in Fig. A and B, compound **S1** located in the well-known binding pocket of MAO-B: benzyloxy group occupies the entrance cavity space, whereas the coumarin moiety binds in the substrate cavity with the pyran ring oxygen pointing toward Tyr326 at the top of the cavity; and a hydrogen bond interaction with Tyr 435 at bottom of the substrate cavity can be observed, which was agreed with the previous report.¹ From Fig. C and D, compared with standard compound **S1**, compound **10e** with the CHO-substituted benzene ring (A) has a similar interactions with MAO-B. Further, compound **10e** not only has a hydrogen bond interaction with Tyr 188, but also has an aromatic π - π stacking interactions with Tyr 398 at bottom of the substrate cavity; The Br-substituted benzyl group occupied the entrance cavity which was a hydrophobic subpocket existing only in the MAO-B isoform and constituted by Leu 171, Ile 316, Tyr 326, Ile 199, Phe 99, Pro 104 and Phe 168.

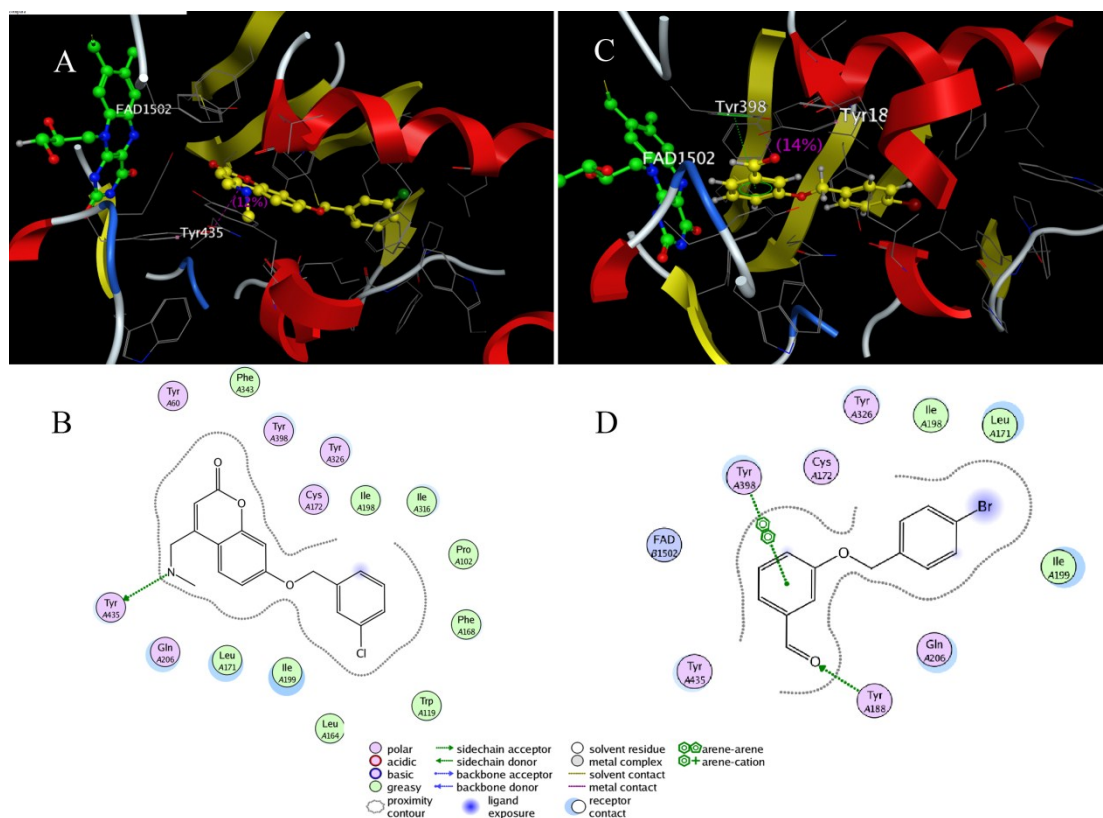


Figure S1. (A) 3D docking model of compound **S1** with *h*MAO-B. Atom colors: yellow-carbon atoms of compound **S1**, gray-carbon atoms of residues of *h*MAO-B, dark blue-nitrogen atoms, red-oxygen atoms. The dashed lines represent the interactions between the protein and the ligand. (B) 2D schematic diagram of docking model of compound **S1** with *h*MAO-B. (C) 3D docking model of compound **10e** with *h*MAO-B. (D) 2D schematic diagram of docking model of compound **10e** with *h*MAO-B.

1. Binda, C.; Wang, J.; Pisani, L.; Caccia, C.; Carotti, A.; Salvati, P.; Edmondson, DE.; Mattevi, A. *J Med Chem.* **2007**, *50*, 5848-5852.